
Magma Mixing in the 1100 AD Montaña Reventada Composite Lava Flow: Interaction of Rift Zone and Central Complex Magmatism

11

Sebastian Wiesmaier, Frances M. Deegan, Valentin R. Troll, Juan Carlos Carracedo, and Jane P. Chadwick

Abstract

Zoned eruption deposits frequently show a lower felsic and an upper mafic member, thought to reflect eruption from a large, stratified magma chambers. In contrast, however, the Montaña Reventada composite flow in Tenerife consists of a lower basanite and a much thicker upper phonolite. A sharp interface separates the basanite and phonolite, and a chilled margin at this contact indicates the basanite was still hot upon emplacement of the phonolite, i.e. the two magmas erupted in very quick succession. Three types of mafic to intermediate inclusions are found in the phonolite, which comprise foamy quenched ones, inclusions with chilled margins and those that are physically mingled, reflecting progressive mixing with a decreasing temperature contrast between the end-member magmas involved. Analysis of basanite, phonolite and inclusions for majors, traces and Sr, Nd and Pb isotopes show the inclusions to be derived from binary mixing of basanite and phonolite end-members in ratios of 2:1–4:1. Although basanite and phonolite magmas were erupted in quick

S. Wiesmaier (✉)
Ludwig-Maximilians-Universität,
Geo- and Environmental Sciences,
Munich, Germany
e-mail: sebastian.wiesmaier@min.uni-muenchen.de

F. M. Deegan
Swedish Museum of Natural History, Laboratory for
Isotope Geology, Stockholm, Sweden

V. R. Troll
Department of Earth Sciences, CEMPEG,
Uppsala University, 75236 Uppsala, Sweden

J. C. Carracedo
Department of Physics (Geology), GEOVOL,
University of Las Palmas, Gran Canaria, Spain

J. P. Chadwick
Science Gallery, Trinity College Dublin,
Dublin 2, Ireland

succession, contrasting $^{206}\text{Pb}/^{204}\text{Pb}$ ratios show them to be genetically distinct. The Montaña Reventada basanite and phonolite first came into contact just prior to eruption and had seemingly limited interaction time. Montaña Reventada erupted from the transition zone between two plumbing systems, the phonolitic Teide-Pico Viejo complex and the basanitic Northwest rift zone. A rift zone basanite dyke most likely intersected a previously emplaced phonolite magma pocket, leading to eruption of geochemically and texturally unaffected basanite, followed by inclusion-rich phonolite that exploited the already established conduit.

11.1 Introduction

Magma mixing occurs when two liquid magmas of distinct composition interact with each other over a defined period of time. However, time-scales of magma mixing may be highly variable and range from hours to tens and hundreds of years. Large ignimbrite eruptions, for instance, have frequently been associated with voluminous stratified magma chambers, in which the compositionally distinct magmas formed over long time-scales from the same parent magma (e.g., Sparks et al. 1977; Blake 1981; Huppert et al. 1982; Wolff and Storey 1984; Blake and Ivey 1986; Freundt and Schmincke 1992; Calanchi et al. 1993; Kuritani 2001; Troll and Schmincke 2002). Alternatively, the origin of mixed magmas has also been explained by the forced intrusion or fountaining of a genetically distinct magma into another, whereby the newly arriving magma may trigger an eruption due to super-heating and re-mobilisation of the previously emplaced, already cooled pocket of magma (e.g., Turner 1980; Campbell and Turner 1986; Turner and Campbell 1986; Eichelberger et al. 2000; Izbekov et al. 2004; Troll et al. 2004). For example, Izbekov et al. (2004) suggested that in 1996, a mafic dyke had dissected a resident andesite magma chamber, triggering the intermittent eruption of a range of mixed products at Karymsky volcano, Kamchatka.

Various mechanisms for the mixing of magmas have been postulated, for example, (1) buoyant rise of mafic magma caused by a density decrease from strong vesiculation, (2) convective stirring or viscous coupling caused by

thermal contrasts between mafic and felsic end-members, (3) forced intrusions of mafic magma into highly viscous and thus more competent felsic magma, and (4) mixing within the conduit during magma ascent (cf. Eichelberger 1980; Bacon 1986; Coombs et al. 2003; Troll et al. 2004; De Campos et al. 2008). The circumstances of magma mixing for a given deposit are thus a result of the dynamics and compositional controls of the related magmatic plumbing system. Key issues for understanding magma mixing are therefore: (a) how long have the compositionally distinct magmas interacted with each other? (b) are these compositionally distinct magmas co-genetic, i.e., derived from the same parental magma? or (c) are they genetically unrelated and met only prior to eruption? This chapter will try to answer these questions through a summary of detailed studies of the compositionally mixed Montaña Reventada lava flow (Araña et al. 1994; Wiesmaier et al. 2011), one of the most recent deposits within the Teide–Pico Viejo succession in Tenerife. At Reventada, a basanite lava flow erupted and was shortly followed by the eruption of phonolite lava from the same vent, thus forming a composite flow or cooling unit. The phonolite part of the flow contains abundant dark inclusions that appear to be related to the basanite part. Earlier studies on Montaña Reventada (Araña et al. 1989, 1994) provided mass balance calculations that, combined with mineral abundances, allowed them to exclude continuous closed system fractional crystallisation as the origin of these inclusions, but supported a hybrid (mixing) origin instead. The lack of mingling textures within the phonolite matrix led the

Fig. 11.1 Picture of Montaña Reventada. Montaña Reventada, the edifice of a complex eruption located in the zone of interaction between the NW rift zone and the central felsic volcanoes Teide and Pico Viejo. This eruption involved mixing of mafic and felsic magmas



authors to believe that the intermediate inclusions formed exclusively through diffusional hybridisation, which would require a long-lived, diffusional interface between basanite and phonolite in the Reventada magma chamber. A long-lived stratified magma chamber, however, is inconsistent with the relatively small volume of the Reventada eruption (0.1 km^3) as thermodynamic considerations indicate that comparably small magma chambers are likely to solidify completely before significant diffusional gradients can develop (cf. Hawkesworth et al. 2000). Equally, the eruption order, i.e., basanite before phonolite, does not agree with common models of stratified magma chambers (Hildreth 1979; Blake 1981; Troll and Schmincke 2002), which are believed to hold the denser magma (here basanite) below the less dense one (here phonolite).

In the study of Wiesmaier et al. (2011), new isotope and geochemical data have been merged with those of Araña et al. (1994), and combined with a detailed textural analysis of inclusion types. This approach resulted in a refined model of magma mixing that is consistent with field and textural constraints and allows for a substantial revision of the magmatic processes ongoing during the Montaña Reventada eruption, with implications for the interaction of distinct magma plumbing systems in Tenerife.

11.2 The Montaña Reventada Lava Flow

Montaña Reventada consists of a small group of vents and associated flow lobes, which have been radiometrically dated at $895 \pm 155 \text{ a BP}$ (Carracedo et al. 2007). Two exceptional roadcuts at 330437/3128642 (UTM 28R $\pm 15 \text{ m}$) at either side of the road TF-38 (locally referred to as “Carretera Boca Tauce-Chío”) provide a cross-section through the complete stratigraphy of this eruption, including the bottom contact with older lavas (Fig. 11.2). This roadcut, at the base of Pico Viejo in the NWRZ, has been previously described by Araña et al. (1994).

The Montaña Reventada stratigraphy comprises the following components from bottom to top: (1) A red basal breccia of about 10–20 cm thickness, composed of scoriaceous basanite, which is scarcely porphyritic and shows flow banding in some clasts. (2) A lower basanite layer of variable thickness (20–200 cm), composed of massive, dark, mainly aphyric lava with flow banding that is frequently folded (Fig. 11.2a). Laterally, the massive parts grade into welded scoria, where the scoria clasts are of variable vesicularity. At 1–2 km downhill from the outcrop described here, the basanite contains abundant plagioclase. (3) An upper phonolite layer of

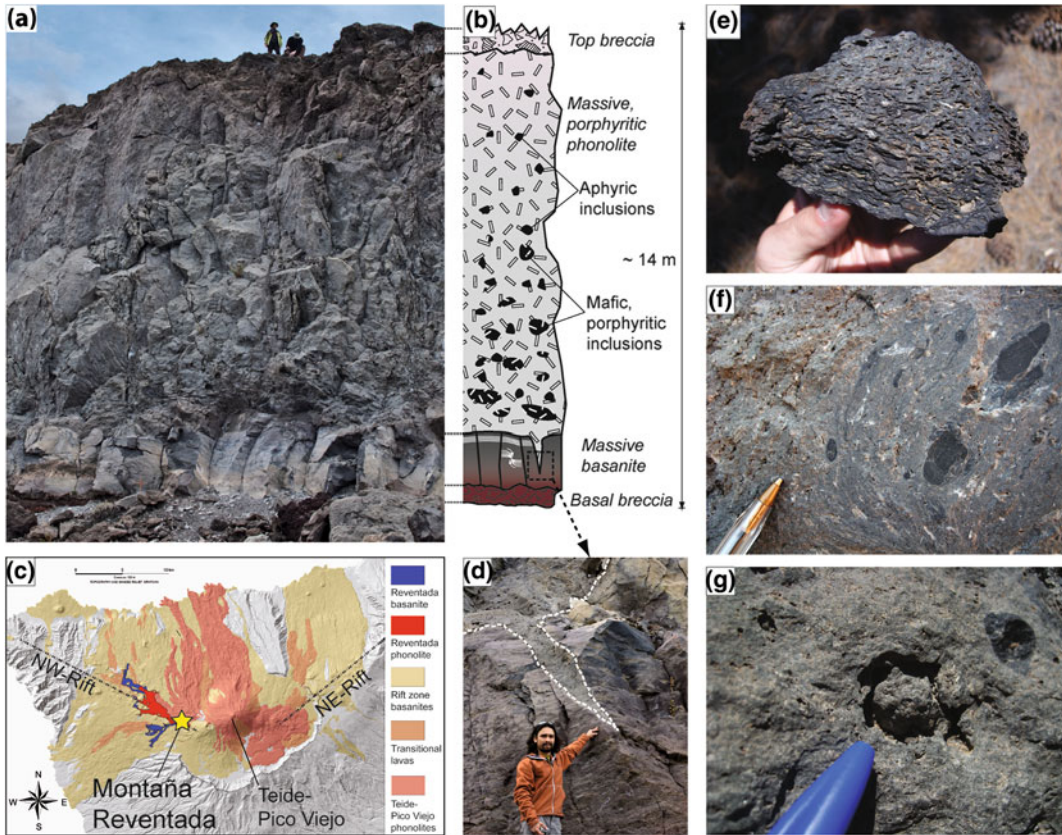


Fig. 11.2 Picture of outcrop and map inset. **a** A photograph of the main outcrop of the Montaña Reventada composite flow with people for scale. **b** A simplified stratigraphic column of this main outcrop. **c** A location map after Carracedo et al. (2007). **d** An opened fracture

within the basanite that has been filled with phonolite. **e** Vesicle-rich and plagioclase bearing basanite can be found at the flow front. **f** Mingled appearance of a light-coloured inclusion. **g** Degassing halo around an inclusion in host phonolite

10–12 m thickness that is massive, light-coloured and porphyritic. The contact between the basanite and the overlying phonolite is sharp and undulating, lacking both top and basal brecciation. In places, the phonolite intrudes the lower basanite or appears to “lift out” basanite blocks (up to 50 cm). At one location, the intruding phonolite caused a chilled margin in the underlying basanite, indicating a considerable temperature contrast (Fig. 11.2d). Within the first metre above the basanite-phonolite contact, vesicles up to 10 cm are abundant. These are elongated parallel to the contact and grade into equant shapes some 40 cm above the contact. The phonolite hosts frequent dark inclusions of varying texture that range in

size from a few cm to 50 cm across and appear to gradually decrease in abundance up-section. The phonolite becomes pink in the uppermost half metre (oxidised top). (4) A top breccia to the phonolite of up to 1.5 m in thickness that consists of large clinker fragments and glassy blocks.

11.3 Research Techniques

To define the lithological units and constrain the processes that gave rise to the Montaña Reventada composite eruption, Wiesmaier et al. (2011) analysed 20 samples from the outcrop for their major- and trace element concentrations as well as

for their Sr, Nd and Pb isotopes. The compositional data are complemented by field and petrographical evidence from the outcrop as well as hand-specimen samples and thin-sections. The sample set comprises 14 whole-rock and six groundmass samples collected from the two road sections at TF-38. Of the whole-rock samples, three basanite, seven phonolite and four inclusion samples were selected for whole-rock analyses and groundmass measurements included two basanite and four phonolite samples.

Results are listed in Table 11.1 with all errors reported as 2SD. A detailed documentation of the analytical methods applied can be found in Wiesmaier et al. (2011).

11.4 Petrological and Geochemical Observations

11.4.1 Petrography

The petrographic description of the samples allows the distinction of basanite, phonolite and in total four different types of mafic inclusions.

11.4.1.1 Basanite

Plagioclase phenocrysts and vesicles are abundant in the flow front of the basanite lava. In contrast, at the outcrop described here, Reventada basanite is essentially aphyric and vesicle-free with only scarce plagioclase phenocrysts. The microcrystalline, melanocratic groundmass consists of lath-shaped plagioclase, pyroxene microlites with high birefringence colours and opaque Fe/Ti-oxides. The groundmass shows abundant flow lamination, which is frequently folded (Fig. 11.3a).

11.4.1.2 Phonolite

The overlying phonolite contains 10 % alkali feldspar, 3 % opaque minerals and scarce clinopyroxene and amphibole with dehydration rims. Feldspar may be intergrown with opaque minerals and/or pyroxene. Feldspar also often displays sieve textures and occurs as single, euhedral crystals with rounded corners and

abundant Carlsbad twinning or, less often, as glomerocrysts of up to 10 mm across.

The microcrystalline, leucocratic phonolite groundmass is holocrystalline and consists mainly of feldspar and opaque minerals. Vesicles are abundant and make up ~10 vol.% of the rock close to the contact with the lower basanite, but this decreases to ~1 vol.% farther away from the basanite (Fig. 11.3c).

11.4.1.3 Inclusions

Inclusion textures range from frothy and vesicle-rich through scarcely porphyritic and banded to porphyritic and mingled. Four major types are distinguished. *Type I*: finely vesicular with a cryptocrystalline groundmass (diktytaxitic texture, cf. Bacon 1986), sometimes containing alkali feldspars with an anhedral relict appearance. This type of inclusion has angular outlines and is occasionally intruded by phonolite and thus appears to have behaved competently against the liquid phonolite magma (Fig. 11.3d, e). *Type II*: dark-coloured, feldspar-bearing inclusions with a lobate, sometimes chilled margin that indicates fluidal behaviour at the time of formation. Type II inclusions contain nodules of darker material (Fig. 11.3f, g). *Type III* inclusions are lighter coloured than type II, are feldspar-bearing and show a coarser-grained groundmass of microlites, feldspars and amphiboles. These inclusions have lobate and diffuse margins (blob-like), and filaments and blobs of dark magma are visible within them. Inclusions of about 1 cm or less in size may show a sharp, well-defined contact, or a diffuse transition between inclusion and phonolite host (Fig. 11.3g, h). Glomerocrysts of feldspar intergrown with opaque oxides, clinopyroxene and amphibole occur. *Type IV*: dense inclusions with scarce feldspar that show flow-banding. Phenocryst orientations generally appear to follow the observed groundmass lamination. The contact to the host phonolite is sharp and angular (Fig. 11.3i).

Feldspars within the inclusions show anorthoclase compositions but also a range of labradorite to oligoclase (Wiesmaier 2010).

Table 11.1 XRF major element and ICP-MS trace element data for Montaña Reventada basanite, inclusion and phonolite samples.

sample:	Basanite					Inclusions					Phonolite	
	205-1	205-2	205-3	205-1 gm	205-2 gm	E 206A	E 206B	E 206D	E 204F	206 Cont		
SiO ₂ (wt%)	46.63	46.2	46.19	46.86	46.71	50.08	50.12	50.44	48.4	57.46		
TiO ₂	3.31	3.35	3.33	3.32	3.36	2.62	2.64	2.6	2.92	1.35		
Al ₂ O ₃	17.16	17.13	17.14	17.18	17.17	17.65	17.68	17.74	17.65	18.49		
Fe ₂ O ₃	11.13	11.22	11.21	11.09	11.19	9.04	9.04	9.02	9.84	5.3		
MnO	0.18	0.18	0.18	0.18	0.18	0.18	0.18	0.18	0.21	0.17		
MgO	4.42	4.53	4.55	4.48	4.58	3.35	3.44	3.39	3.75	1.46		
CaO	9	9.15	9.12	9.06	9.14	6.91	7.01	6.89	7.72	2.89		
Na ₂ O	4.94	4.97	4.93	4.83	4.86	6.3	6.05	6.07	5.67	7.59		
K ₂ O	1.92	1.85	1.88	1.91	1.91	2.46	2.62	2.66	1.75	4.32		
P ₂ O ₅	1.26	1.29	1.3	1.29	1.29	0.99	1	1	1.17	0.4		
H ₂ O	0.08	0.09	0.09	–	–	0.12	0.14	0.08	0.24	0.17		
CO ₂	0.02	0.02	0.02	–	–	0.02	0.02	0.01	0	0.04		
Sum	100.28	100.17	100.13	100.51	100.7	99.91	100.1	100.29	99.45	99.69		
Ba (ppm)	581.9	728.4	528.8	526.1	616.2	780.3	594.6	708.7	1053.7	668.5		
Sr	982.1	1327.3	936.7	910.3	1068.2	968.5	767.4	885.2	1075.5	239.6		
Hf	7.04	8.53	5.95	6.29	7.32	8.28	6.65	8.43	6.53	7.68		
Th	6.48	8.59	6.32	5.59	7.21	11.07	7.68	11.09	6.36	8.97		
U	1.90	2.19	1.55	1.68	1.86	2.43	2.00	2.49	1.59	2.79		
Nb	82.3	115.3	77.5	81.3	99.8	113.4	93.3	110.3	110.8	113.8		
Ta	5.75	7.20	4.63	4.87	5.54	7.07	5.64	6.74	6.05	6.41		
Rb	39.50	36.31	29.89	36.00	33.18	58.16	47.98	53.57	25.93	64.70		
Pb	3.52	4.09	2.88	3.18	3.62	5.43	4.12	5.32	3.53	5.53		
²⁰⁶ Pb/ ²⁰⁴ Pb	19.7418(16)	19.7401(10)	19.7355(7)	19.7377(9)	19.7193(10)	19.7641(12)	19.7528(7)	19.7594(7)	19.7660(8)	19.7671(9)		
²⁰⁷ Pb/ ²⁰⁴ Pb	15.6122(17)	15.6163(9)	15.6213(9)	15.6173(16)	15.6146(17)	15.6196(15)	15.6117(8)	15.6175(8)	15.6142(9)	15.6168(15)		
²⁰⁸ Pb/ ²⁰⁴ Pb	39.5607(31)	39.5673(20)	39.5720(14)	39.5638(18)	39.5423(22)	39.5858(23)	39.5603(15)	39.5786(14)	39.5701(16)	39.5769(19)		

(continued)

Table 11.1 (continued)

sample:	Basanite										Inclusions										Phonolite	
	206-2	206-3	206-5	206-2 gm	206-5 gm	207-4	207-5	207-6	207-4 gm	207-6 gm	206-2	206-5	206-2 gm	206-5 gm	207-4	207-5	207-6	207-4 gm	207-6 gm	207-4 gm	207-6 gm	
SiO ₂ (wt%)	58.68	59.12	57.65	59.31	57.82	58.88	58.17	58.75	59.16	58.86	58.58	58.88	57.82	58.88	58.17	58.75	59.16	58.86	58.86	59.16	58.86	
TiO ₂	1.08	1.03	1.28	1.06	1.28	1.1	1.21	1.12	1.08	1.11	1.11	1.21	1.28	1.21	1.21	1.12	1.08	1.11	1.08	1.11	1.11	
Al ₂ O ₃	18.53	18.61	18.58	18.63	18.52	18.58	18.5	18.51	18.55	18.47	18.58	18.58	18.52	18.58	18.5	18.51	18.55	18.47	18.55	18.47	18.47	
Fe ₂ O ₃	4.56	4.41	5.09	4.54	5.09	4.54	4.99	4.57	4.53	4.76	4.54	4.99	5.09	4.54	4.99	4.57	4.53	4.76	4.53	4.76	4.76	
MnO	0.16	0.16	0.17	0.16	0.17	0.17	0.16	0.16	0.17	0.17	0.17	0.16	0.17	0.17	0.16	0.16	0.17	0.17	0.17	0.17	0.17	
MgO	1.05	1	1.33	1.04	1.35	1.09	1.28	1.12	1.06	1.12	1.09	1.28	1.35	1.09	1.28	1.12	1.06	1.12	1.06	1.12	1.12	
CaO	1.99	1.87	2.65	1.97	2.63	1.98	2.35	2.1	1.96	2.08	1.98	2.35	2.63	1.98	2.35	2.1	1.96	2.08	1.96	2.08	2.08	
Na ₂ O	7.91	7.85	7.7	7.9	7.64	7.67	7.67	7.81	7.73	7.88	7.67	7.67	7.64	7.67	7.67	7.81	7.73	7.88	7.73	7.88	7.88	
K ₂ O	4.75	4.81	4.42	4.82	4.52	4.73	4.57	4.66	4.83	4.74	4.73	4.57	4.52	4.73	4.57	4.66	4.83	4.74	4.83	4.74	4.74	
P ₂ O ₅	0.29	0.28	0.37	0.29	0.38	0.29	0.35	0.31	0.29	0.32	0.29	0.35	0.38	0.29	0.35	0.31	0.29	0.32	0.29	0.32	0.32	
H ₂ O	0.09	0.1	0.09	-	-	0.16	0.26	0.2	-	-	0.16	0.26	-	0.16	0.26	0.2	-	-	-	-	-	
CO ₂	0	0	0.01	-	-	0.02	0.01	0.02	-	-	0.02	0.01	-	0.02	0.01	0.02	-	-	-	-	-	
Sum	99.24	99.4	99.5	99.98	99.67	99.29	99.52	99.37	99.6	99.76	99.29	99.52	99.67	99.29	99.52	99.37	99.6	99.76	99.6	99.76	99.76	
Ba (ppm)	996.9	1289.7	881.1	789.1	796.4	975.8	1055.4	1032.9	839.8	694.3	789.1	1055.4	796.4	975.8	1055.4	1032.9	839.8	694.3	839.8	694.3	694.3	
Sr	186.7	218.4	274.0	154.2	270.4	171.3	244.7	203.0	159.1	155.6	154.2	244.7	270.4	171.3	244.7	203.0	159.1	155.6	159.1	155.6	155.6	
Hf	10.86	13.18	9.35	10.79	10.71	9.59	10.07	9.31	11.10	7.83	10.79	10.07	10.71	9.59	10.07	9.31	11.10	7.83	11.10	7.83	7.83	
Th	14.90	19.87	12.27	12.45	12.57	13.99	15.06	11.83	14.87	10.63	12.45	15.06	12.57	13.99	15.06	11.83	14.87	10.63	14.87	10.63	10.63	
U	3.71	4.68	3.28	3.29	3.49	3.58	3.73	2.75	3.75	2.33	3.29	3.73	3.49	3.58	3.73	2.75	3.75	2.33	3.75	2.33	2.33	
Nb	157.8	192.1	134.4	157.3	164.4	146.6	157.8	162.0	165.1	121.8	157.3	157.8	164.4	146.6	157.8	162.0	165.1	121.8	165.1	121.8	121.8	
Ta	8.75	10.39	7.51	8.14	8.20	8.28	8.17	7.85	8.43	6.01	8.14	8.17	8.20	8.28	8.17	7.85	8.43	6.01	8.43	6.01	6.01	
Rb	101.62	116.55	79.90	91.25	95.38	90.05	97.71	86.14	91.28	62.88	91.25	97.71	95.38	90.05	97.71	86.14	91.28	62.88	91.28	62.88	62.88	
Pb	8.91	10.93	7.34	8.18	7.93	8.27	8.57	6.75	8.67	5.25	8.18	8.57	7.93	8.27	8.57	6.75	8.67	5.25	8.67	5.25	5.25	
²⁰⁶ Pb/ ²⁰⁴ Pb	19.7807(11)	19.7762(6)	19.7746(6)	19.7723(6)	19.7708(10)	19.7767(8)	19.7761(7)	19.7802(7)	19.7723(10)	19.7750(12)	19.7746(6)	19.7767(8)	19.7708(10)	19.7767(8)	19.7761(7)	19.7802(7)	19.7723(10)	19.7750(12)	19.7723(10)	19.7750(12)	19.7750(12)	
²⁰⁷ Pb/ ²⁰⁴ Pb	15.6232(14)	15.6175(9)	15.6189(8)	15.6178(8)	15.6195(15)	15.6219(10)	15.6210(9)	15.6210(9)	15.6203(16)	15.6209(17)	15.6189(8)	15.6219(10)	15.6195(15)	15.6219(10)	15.6210(9)	15.6210(9)	15.6203(16)	15.6209(17)	15.6203(16)	15.6209(17)	15.6209(17)	
²⁰⁸ Pb/ ²⁰⁴ Pb	39.5997(23)	39.5845(14)	39.5882(13)	39.5835(14)	39.5843(22)	39.5980(18)	39.5929(14)	39.5983(15)	39.5873(22)	39.5931(25)	39.5882(13)	39.5980(18)	39.5843(22)	39.5980(18)	39.5929(14)	39.5983(15)	39.5873(22)	39.5931(25)	39.5873(22)	39.5931(25)	39.5931(25)	

Major and trace element and Pb isotope data for Montaña Reventada. Samples with number 205 are from the basanite. 206 Cont is the phonolite sample just above the contact between basanite and phonolite. Samples with number 207 are from the top of the phonolite layer and 206 samples are from the bottom of the phonolite. "gm" in a sample name denotes a groundmass sample

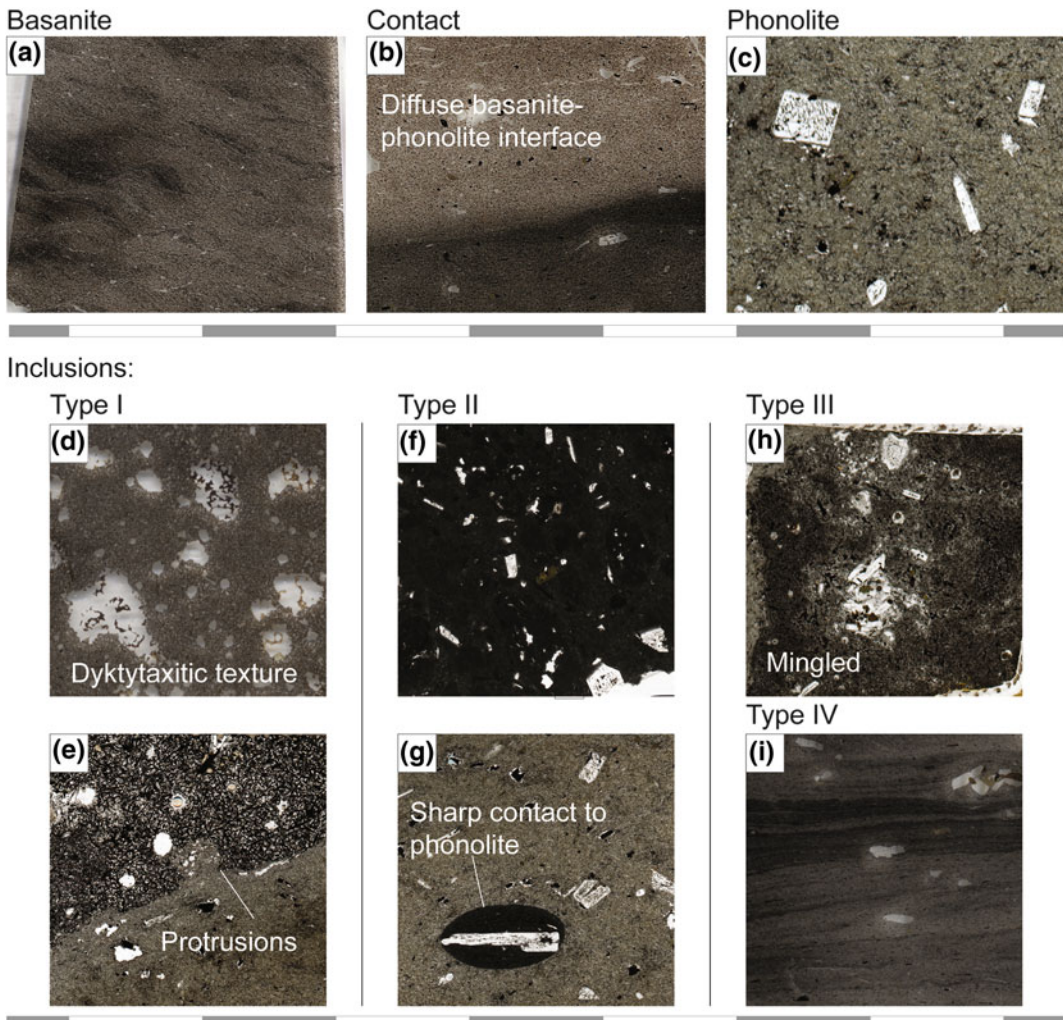


Fig. 11.3 Photomicrographs and scans of thin-sections. Thin-section images of Montaña Reventada rocks (scans: a, b, d, i; photomicrographs: c, e, f, g, h). **a** basanite, **b** diffuse contact between basanite and phonolite, **c** phonolite, **d–e** type I inclusions, frothy and vesicle-rich,

f–g type II inclusions, crystal-rich and possessing a chilled margin, **h** type III inclusions massive, crystal-rich, and mingled, **i** type IV inclusions, flow-banded. Scale bar in 1 cm divisions. Sieve-textured feldspar occurs in all samples

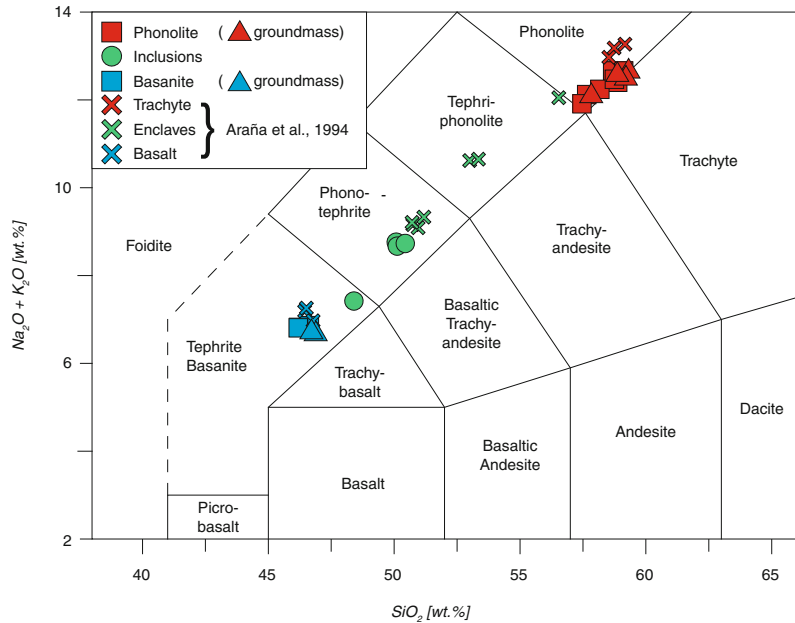
11.4.2 Whole-Rock and Groundmass Composition

11.4.2.1 Major Elements

In the Total Alkali versus Silica diagram (TAS; Le Bas et al. 1986), the lower lava layer classifies as basanite and the upper one as phonolite, while inclusions contained within the phonolite represent variable compositions between the two, plotting as either basanite,

phonotephrite or tephriphonolite (Table 11.1, Fig. 11.4). Inclusion data from Araña et al. (1994) plot in the same linear array between basanite and phonolite, with higher alkali element and silica concentrations. In fact, all major element data form linear trends between basanite and phonolite and the gap between the two principal lava types is always bridged by inclusions of intermediate composition from both data sets (Fig. 11.5).

Fig. 11.4 TAS diagram. Total alkali versus silica diagram after Le Bas et al. (1986). The two principal lava types, basanite and phonolite, are end-members, while the inclusions are of variable intermediate compositions. The data of Araña et al. (1994) (crosses) plot on the same linear trend as the samples from Wiesmaier et al. (2011), between the two principal lava compositions



11.4.2.2 Trace Elements

In a multi-element variation diagram normalised to primitive mantle, basanite and inclusion samples show comparable patterns, apart from the Large Ion Lithophile Elements (LILE) Cs, Rb and Ba and the High Field Strength Elements (HFSE) Th and U, in which inclusions appear more enriched. Phonolite samples are more enriched than basanite in the LILE, but display a pronounced negative Sr and positive Zr anomaly and an overall depletion in MREE (Table 11.1).

When whole-rock trace element data are plotted against Zr concentration as an index of differentiation (cf. Wolff et al. 2000), basanite and phonolite samples again plot as end-members, with the inclusions generally filling the space in-between. However, phonolites show a rather widespread array in several incompatible trace elements, while the basanites appear closely spaced.

11.4.2.3 Isotope Data

Basanite whole-rocks have $^{87}\text{Sr}/^{86}\text{Sr}$ values of between 0.703032(9) and 0.703040(7) (groundmass: 0.703024(10) to 0.703046(9)). The phonolite whole-rocks range from 0.703032(7) to

0.703062(9) (groundmass: 0.703032(9) to 0.703082(7)). The inclusions display values from 0.703032(7) to 0.703059(9).

Basanites show $^{143}\text{Nd}/^{144}\text{Nd}$ ratios from 0.512855(38) to 0.512896(46) and phonolites from 0.512848(42) to 0.512910(46). Inclusions show a range in Nd ratios between 0.512871(46) and 0.512899(42). All Nd ratios are within error of each other.

The $^{206}\text{Pb}/^{204}\text{Pb}$ ratios range from 19.7193(21) to 19.7418(31) versus 19.7528(14) to 19.7660(16) versus 19.7671(18) to 19.7807(23), for basanite, inclusions and phonolite, respectively, with significant differences among these three groups. In contrast however, basanite, inclusion and phonolite samples overlap in their $^{207}\text{Pb}/^{204}\text{Pb}$ ratios (15.6122(34) to 15.6213(17) versus 15.6117(17) to 15.6196(29) versus 15.6168(30) to 15.6232(28), respectively). The $^{208}\text{Pb}/^{204}\text{Pb}$ ratios partially overlap between basanite, inclusions and phonolite (39.5423(43) to 39.5720(29) versus 39.5603(29) to 39.5858(46) versus 39.5769(39) to 39.5997(45), respectively), but with each group reaching higher values. The results for Sr, Nd and Pb isotopes agree well with existing data for Tenerife igneous rocks (Palacz

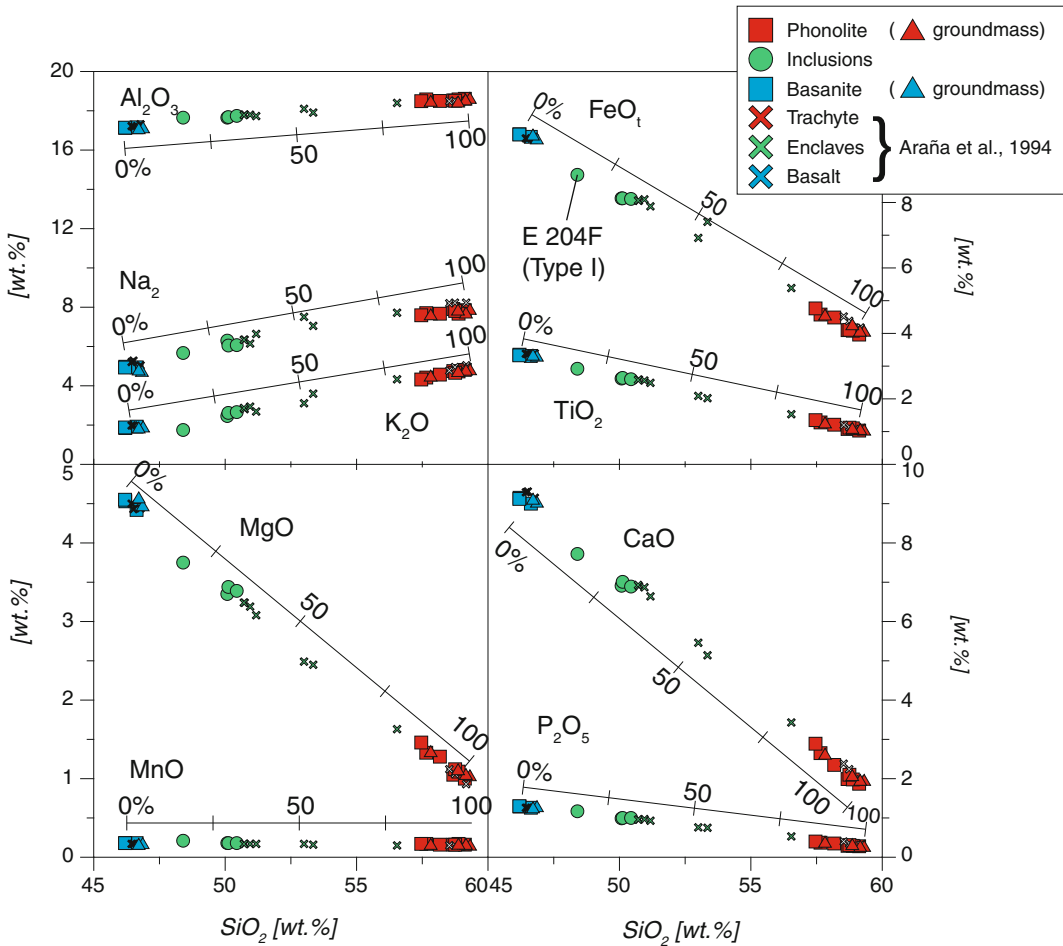


Fig. 11.5 Harker diagrams with graphical mixing solution. Whole-rock major element composition of the Montaña Reventada eruption. Fe data recalculated to FeO_{tot} using the formula $\text{FeO}_{\text{tot}} = \text{FeO} + 0.899 \text{Fe}_2\text{O}_3$ (Bence and Albee 1968). All major elements define straight trends when correlated to SiO_2 , which indicates

the origin of the inclusions to be mixing of the two principal components basanite and phonolite, rather than by fractional crystallisation. Note graphical mixing lines that indicate the percentage of phonolite material for intermediate compositions

and Wolff 1989; Simonsen et al. 2000; Abratis et al. 2002; Gurenko et al. 2006). All errors are reported as 2SD (Table 11.1).

11.5 Emplacement and Formation of the Montaña Reventada Lava Flow

11.5.1 Subaerial Emplacement of Lava

Several lines of evidence allow us to establish that the basanite and phonolite were part of the

same eruption. Firstly, the focus will be on the eruption dynamics at the surface.

The basanite shows a chilled margin where the phonolite intruded (Fig. 11.2d), implying that the basanite was still hot at the time the much cooler phonolite came in contact with it. Further evidence for this is the vesiculation of the phonolite, which is limited to a zone of one metre upwards from the basanite-phonolite contact. This localised zone of vesicles is probably the result of inclusions that were reheated at atmospheric pressure within the phonolite and which

consequently liberated volatiles (see inclusion degassing halos in Fig. 11.2g). The basanite and the phonolite are thus effectively contemporaneous. Only an underlying basanite that was still hot can have caused the inclusions to decompose and develop a chilled margin.

The sharp contact in-between basanite and phonolite holds further clues to the emplacement process. Common 'a'ā lava flows form by developing a chilled crust against the air which brecciates and gives an 'a'ā flow its characteristic rugged surface appearance. During flow, this brecciated top is continuously transported to the flow front, where it rolls onto the ground (Merle 1998) and is consequently run over by the proceeding lava. As a result, the standard stratigraphy of an 'a'ā lava flow consists of a basal breccia, a massive inner part and a top breccia (Cas and Wright 1987).

However, at Montaña Reventada, the contact between basanite and phonolite is sharp, i.e., the basanite lacks a top breccia and the phonolite lacks a bottom breccia. The missing breccias are either not preserved or have never formed. However, the type IV inclusions (massive, flow-banded and angular) closely resemble the laminated texture of the underlying basanite, hence, they have most likely been picked up by the phonolite while overriding the basanite. It thus seems likely that the phonolite rafted on top of the ductile basanite, at least in the area of the outcrop. Rafting would allow it to erode the basanite top breccia and pick up the breccia clasts while not developing its own bottom breccia. The lack of a top basanite breccia and bottom phonolite breccia therefore provides further evidence in support of the two magmas of Montaña Reventada having been emplaced almost simultaneously.

11.5.2 Origin of Inclusions

11.5.2.1 Major and Trace Element Constraints

Whole-rock major element trends are linear for all oxide data from both Araña et al. (1994) and Wiesmaier et al. (2011). Together they form a semi-continuous compositional sequence, with

intermediate inclusions bound by the basanite and phonolite end-member compositions (Fig. 11.5). As the major element patterns are exclusively straight, lacking the typical kinks expected from fractional crystallisation (cf. Geldmacher et al. 1998), physical and chemical mingling and mixing are thought to be the dominant processes active during formation. Such straight trends should not be confused with the much more complex and fluctuating geochemical trends that are produced by the diffusive gradients between two magmas. Although these diffusive gradients are the fundamental driver of mixing and homogenisation, they occur on diffusion distances of sub-cm scale and in single samples only (De Campos et al. 2008). However, for analysis each sample has to be homogenised, including those that show various degrees of magma mixing. As a result complex S-shaped diffusional trends are not preserved and the analysis of a sample suite will produce straight mixing trends, such as observed at Reventada. Alternatively, inclusions may have been thoroughly hybridised when still liquid, so that straight geochemical trends may also be interpreted to reflect an advanced stage of mixing. The straight trends observed at Montaña Reventada thus point towards a mixing origin for the mafic inclusions that are found in the phonolite.

These straight mixing trends allow calculation of the proportions of each component involved during the mixing process. Trace element and major element oxide concentrations in inclusions were modelled as two-component bulk mixtures of basanite and phonolite and the respective maximum and minimum concentrations found for each major and trace element were used.

For most major and trace elements, the inclusions can be equated to mixtures of between 66:34 basanite to phonolite (E206A, E206B and E206D) and 80:20 basanite to phonolite (E204F). This agrees well with graphical mixing solutions in the Harker diagrams, where the three inclusions (E206A, E206B and E206D) cluster together but the latter (E204F) shows a slightly more mafic composition (Fig. 11.5).

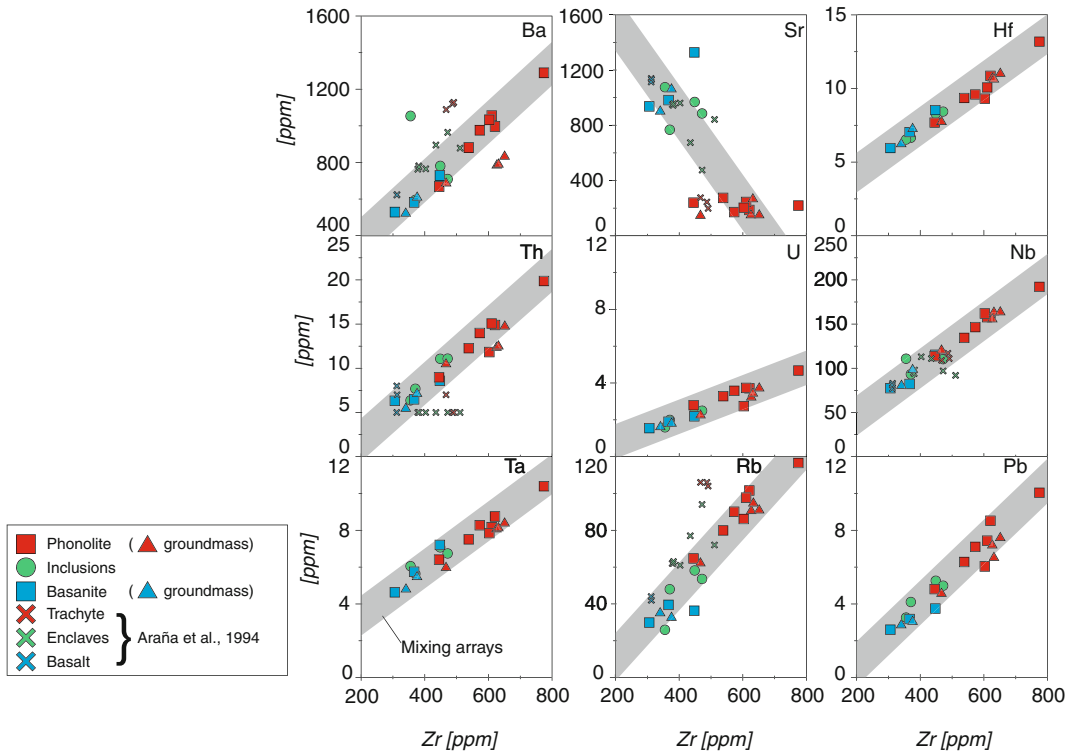


Fig. 11.6 Matrix of trace element plots. Selected trace elements are plotted versus Zr concentration. The crosses denote data from Araña et al. (1994) for comparison. Note the linear variation among the sample suite in most trace elements. Ba, Sr and Rb may be affected by crystal

transfer of feldspar between the end-member magmas, the dominant mineral phase at Montaña Reventada. Phonolite samples show a wide spread in trace element concentrations, which is possibly a result of diffusional hybridisation

Two-component bulk mixing of basanite and phonolite yields matches for the major oxides SiO_2 , MgO , Fe_2O_3 and TiO_2 . The two major element oxides MnO and P_2O_5 are within 0.01 wt% of the model limits, which we deem a satisfactory fit. Most trace elements are modelled satisfactorily too.

Deviations in element concentrations from ideal mixing behaviour are few and can be well explained by diffusive phenomena. Slightly lower K_2O concentrations than expected may indicate uphill diffusion of K_2O towards the phonolite (cf. Watson and Baker 1991; Bindeman and Perchuk 1993; Araña et al. 1994; Bindeman and Davis 1999), which would be in line with the enhanced diffusivities of this element (Walker et al. 1981; Watson 1982; Walker

and DeLong 1982; Leshner 1986; Leshner and Walker 1986). The higher than expected concentration of Al_2O_3 and Na_2O in all inclusions is, in turn, suggestive of anorthoclase added from the phonolite magma (Fig. 11.6).

Trace elements that deviate by more than 10 % from the linear two-component bulk mixing interval are mainly the lithophile elements Li, Sc, Cs, Rb and U. These elements are depleted in inclusions, which can also be explained by uphill diffusion, previously recognised for Li, Cs and Rb in basalt–rhyolite systems (Bindeman and Davis 1999). The siderophile element Ni and the chalcophile element Cu are also depleted in the inclusions with respect to the mixing calculation (Table 11.2). Barium, in turn, is enriched in the type I inclu-

Table 11.2 Modelling of inclusion compositions.

Inclusion	Basanite (%)	Phonolite (%)	Compared with calculated mixture	
			Enriched in:	Depleted in:
E206A	66	34	–	Li, Cu
E206B	66	34	–	Sc, Cu
E206D	66	34	–	–
E204F	80.4	19.6	Ba	Ni, Cu, Cs, Rb, U

Percentages of two-component bulk mixtures between basanite and phonolite that reproduce inclusion compositions. Some trace elements were enriched or depleted in the real samples compared to the theoretical mixture, but variations remain unique to each sample

sion E204F, which may be explained by the addition of Ba-rich anorthoclase from Montaña Reventada phonolite.

In summary, the majority of major and trace elements agree with the ideal mixing trend and apparent deviations are in line with well-documented diffusive or accumulative mechanisms.

11.5.2.2 Isotope Fingerprinting of Basanite, Phonolite and Inclusions

Although the inclusions occupy intermediate values between basanite and phonolite, all three rock types overlap within their analytical uncertainty in Sr and Nd isotopes (not shown) and are thus indistinguishable from each other for these components. The Pb isotopes, however, show distinct $^{206}\text{Pb}/^{204}\text{Pb}$ signatures for basanite and phonolite. The basanites, phonolites and inclusions show similar $^{207}\text{Pb}/^{204}\text{Pb}$ ratios, but systematic variation in $^{206}\text{Pb}/^{204}\text{Pb}$. An implication of the significant difference in the observed Pb isotope ratios between basanite and phonolite is that they cannot be co-genetic. This is consistent with the recent phonolite eruptions from the Teide-Pico Viejo central complex incorporating variable amounts of crustal components, i.e. they are likely isotopically distinct from the rift zone basanites that are comparatively free from crustal assimilation (Chap. 10).

The distinct Pb isotope signatures of basanite and phonolite also allow testing whether or not the inclusions are intermediate to these end-members. From the dataset ($n = 20$), all inclusion samples can be explained as isotopic mixtures between the basanite and phonolite

end-members. This divides the components of Montaña Reventada into three arrays, with the mafic to intermediate inclusions placed in-between the basanite and phonolite (Fig. 11.7). The magmatic inclusions are therefore direct evidence of basanite–phonolite interaction at depth. In the next section, a detailed textural analysis of these inclusions will help to decipher the magma chamber configuration and the mechanism that led to mixing of the two end-member magmas.

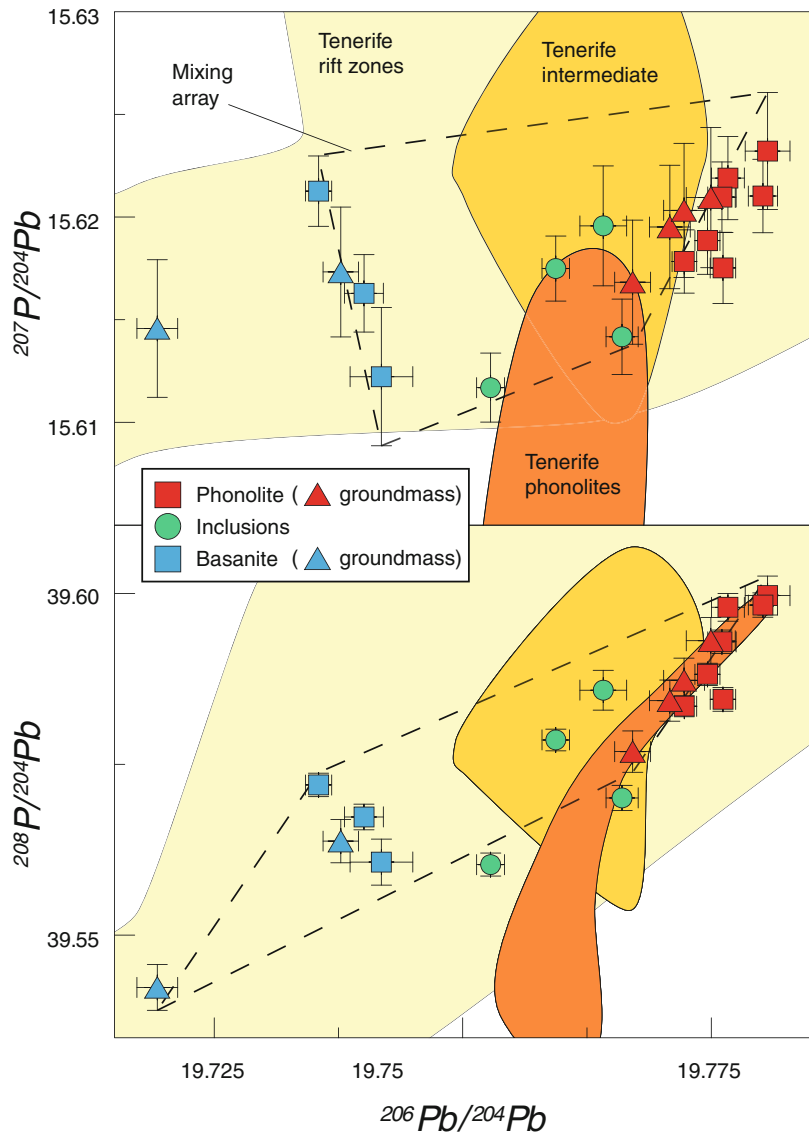
11.5.3 Subsurface Dynamics

Altogether four types of inclusions were recorded in the Reventada phonolite. Since the following discussion is concerned with processes at depth prior to and during eruption, type IV inclusions, which have been identified as pick-up clasts, i.e. as subaerially solidified rocks, will not be mentioned here. The remaining inclusion types, I through III, record a progressive sequence of basanite-phonolite interaction, reflecting a continuous interaction while temperature differences between the end members gradually disappear.

11.5.3.1 Type I Inclusions

Type I inclusions in the Montaña Reventada phonolite are angular fragments of a vesicle-rich “mafic foam” (a term coined by Eichelberger 1980), indicating that a large temperature contrast must have led to rapid crystallisation of the hotter, mafic magma (cf. Bacon and Metz 1984; Bacon 1986). The resultant exsolution of volatiles in the residual melt raises the melt’s

Fig. 11.7 Pb isotope plot. Pb-Pb isotope systematics of the Montaña Reventada eruption. Errors are 2SD. Fields denote existing data from the Tenerife Teide-Pico Viejo complex and rift zones (Wiesmaier 2010): in yellow primitive rift zone basanites, in orange intermediate rocks and in red phonolites. Basanite and phonolite data from this study define independent sub-vertical trends. Mafic to intermediate inclusions that are found in the phonolites show a similar range in $^{207}\text{Pb}/^{204}\text{Pb}$ but bridge the gap in $^{206}\text{Pb}/^{204}\text{Pb}$ between the basanite and phonolite, consistent with a mixing origin. The basanite and phonolite end-members, in turn, define two parallel trends that do not overlap, characterising them as two genetically distinct magmas that define a mixing array



solidus and hence enhances solidification in the residual melt (cf. Sparks et al. 1977; Hammer et al. 2000). The result is a boundary layer of foamy, vesiculated material that is interpreted to form upon initial contact of hot, mafic with cool, felsic magma (Eichelberger 1980) and we interpret type I inclusions accordingly. By implication, the phonolite was probably rather cool when the basanite first arrived, but must have been conductively heated by the basanite. The initially quenched and almost solid, vesicular boundary zone was subsequently disrupted,

creating the angular fragments of type I inclusions and allowing for direct contact between the liquid portions of the basanite with the heated phonolite magma.

11.5.3.2 Type II Inclusions

In comparison to type I inclusions, type II inclusions are indicative of a lesser, but still considerable temperature contrast. Instead of the angular outlines characteristic of type I inclusions, the smooth and undulate contacts of type II inclusions resemble liquid blobs and show that

the basanite was at some point able to undergo ductile deformation. The temperature difference between the two bodies of magma was still sufficiently large to cause chilled margins (cf. Sparks et al. 1977; Eichelberger 1980; Marshall and Sparks 1984). The two magmas were therefore far from thermal equilibrium, which implies a close temporal relationship between the formation of type I (mafic foam) and type II inclusions. Type II inclusions are interpreted to result from entrainment of mafic magma into reheated and hence re-mobilised phonolite magma. Type II inclusions have thus likely formed after the initial contact zone had been disrupted to form type I inclusions (cf. Troll et al. 2004).

11.5.3.3 Type III Inclusions

Type III inclusions are a lighter colour, with filaments and blobs of darker, mafic magma within them (see Fig. 11.2f). Physical mixing (mingling) of two liquids results in active regions of intense mingling (filaments), and coherent regions largely unaffected by mingling (blobs) (Perugini et al. 2003). The banded textures of type III inclusions demonstrate that a phase of mingling occurred at some point during basanite-phonolite interaction. To allow such intimate mingling, a reduced viscosity contrast must have prevailed between basanite and phonolite (cf. Jelinek et al. 1999), otherwise all other inclusion types ought to show comparable filament textures. The filaments and blobs in type III inclusions are thus most probably the result of intense physical mingling of cooled basanite and heated-up phonolite, i.e. magmas of similar or near-identical viscosities (cf. Perugini et al. 2003). Further evidence for reheating of phonolite is provided by sieve textures in anorthoclase crystals, which are interpreted to originate by remelting of the crystal (cf. Hibbard 1995; Stewart and Pearce 2004). As such, type III inclusions are indicative of advanced thermal equilibration between basanite and phonolite, which makes them the youngest inclusions to have formed during interaction of these two magmas.

This mirrors the results of several studies that have suggested that magma mixing is a

progressive interplay of initially dominant mingling and successively more important diffusion (e.g., Kouchi and Sunagawa 1985; Perugini et al. 2003; Zimanowski et al. 2004).

To achieve hybridisation of two magmas within a short timeframe, it is vital that intense physical mingling takes place first. Type III inclusions are thus interpreted to be the result of physical interaction between the basanite and the phonolite magma, suggesting that the interaction was not limited to diffusive hybridisation as suggested by Araña et al. (1994), but was locally associated with intense physical mixing. The succession of type I through III inclusions thus indicates the progressive interaction of two magmas that were initially distinct in composition, temperature and viscosity. Upon interaction, they began to thermally equilibrate and approached each other in their viscosities to allow progressive hybridisation.

11.5.4 Timescale of Basanite-Phonolite Interaction

The preservation of textural transitions in the inclusions from initial formation of mafic foam through quenching and chilled margin development to final liquid-liquid interaction indicates a rapid succession of events. The formation of chilled margins in type II inclusions must have swiftly followed the initial quench-type inclusions in type one inclusions, for the thermal contrast between basanite and phonolite to still be strong enough to allow chilled margins to form. The transition between type II and type III inclusions is less clear, but a close temporal relationship is likely. By using the MELTS algorithm in combination with cooling and decompression experiments, Coombs et al. (2003) temporally constrained the formation of inclusions and chilled margins between an andesite and a dacite to be on the order of hours only. The duration of mixing at Montaña Reventada was therefore probably on a similar order of magnitude (hours to days).

This has implications for the configuration of the magma chamber at depth, because short interaction between basanite and phonolite on

the order of few hours is inconsistent with the concept of a long-lived, stratified magma chamber, in which compositionally distinct magmas develop by magmatic differentiation for decades prior to eruption as postulated by Araña et al. (1994). Such a compositionally stratified body of magma is thought to possess stable, diffusive gradients between distinct magmas. In such a magma chamber, quenched material, like that found at Montaña Reventada, is less likely to form because thermal gradients are smooth.

Furthermore, the groundmass of both basanite and phonolite appear to be relatively free of physical mixing; it is only the inclusions that are the result of magma mixing. The total volume of mixed inclusions therefore is restricted at Reventada, with inclusions estimated to amount to less than 1 vol.% of the total deposit volume (Araña et al. 1994). Mingling of basanite and phonolite appears to have been confined to a spatially small zone of interaction, and took place after an initial carapace of quenched basanite (mafic foam) had been disaggregated. In order to efficiently mix two magmas, their viscosities need to be comparable and it has been suggested that only thermal equilibration may reasonably cause approaching viscosities (Campbell and Turner 1986). According to these authors, this may occur either in long-lived, stratified magma chambers or as a spatially restricted phenomenon during fountaining or forced intrusion, creating a small-volume, hybrid boundary layer between mafic and felsic magma. Since at Montaña Reventada a rather short period of interaction is indicated and a relatively small volume of hybrid inclusions is observed within the host phonolite, Wiesmaier et al. (2011) postulated a forced intrusion of basanite into an ambient body of phonolite magma.

11.5.5 Mixing Mechanism

In the previous section it was shown that basanite and phonolite likely interacted over a short time-scale by means of a forced intrusion of basanite into phonolite. The following discussion will now establish the detailed

mechanism(s) by which the basanite and phonolite mingled to produce the observed range of hybrid inclusions. Viscous coupling has been suggested in a comparable case in which the mafic member of an eruption was emplaced before the felsic one. Pinatubo erupted andesite before dacite in 1991, the latter of which comprises the bulk of the final deposit (Pallister et al. 1992). Snyder and Tait (1996) tested the Pinatubo scenario experimentally by using the viscous coupling of magmas driven by thermal convection (after Huppert et al. 1983, 1984). It was found that a strong temperature contrast between mafic and felsic magma may trigger local convection within the felsic member, thereby entraining mafic liquid by viscous coupling. Their mafic magma analogue liquid reached the roof of the chamber as a mixed layer, thus providing a model for the eruption of mixed andesite erupting before pristine dacite (as at Pinatubo in 1991).

The Pinatubo model, however, does not satisfactorily explain the situation at Reventada. First of all, at Pinatubo hardly any quenched inclusions have been found, whereas at Reventada these type I and type II inclusions are ubiquitous, indicating a larger temperature contrast between basanite and phonolite compared to andesite and dacite. Furthermore, the first-erupting andesite at Pinatubo is of hybrid origin followed by a pristine dacite, while at Reventada the situation is reverse; the basanite appears texturally and compositionally pristine. Viscous coupling may thus not be the driving mechanism for magma mixing at Montaña Reventada.

In turn, Reventada phonolite, i.e., the later erupted magma, is indeed affected by mixing demonstrated by the inclusions that originate from initial contact between the two magmas. It appears that the phonolite collected the leftover basanite material that had initially quenched against the phonolite. Two possible configurations of interaction were thus suggested. Either the basanite was able to largely bypass the phonolite chamber at its side and only tap it peripherally, or the basanite formed a dyke through the phonolite, being shielded from interaction by the early-formed quench horizon.

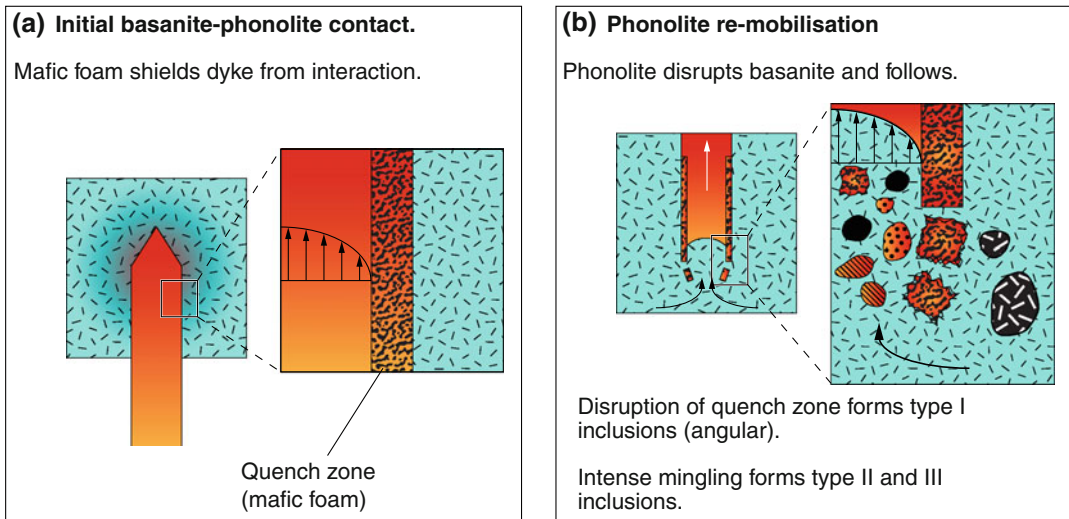


Fig. 11.8 Quench sequence of basanite and phonolite. Schematic representations of the immediate contact between basanite and phonolite. **a** At first contact between basanite and phonolite, the basanite develops a vesicular, solid layer of quenched material (mafic foam) that isolates the bulk of the basanite from interaction with the phonolite. However, the lifespan of

this screen of quenched material may be short. **b** Both magmas equilibrate thermally, thus remobilising the phonolite. After the basanite eruption wanes, the phonolite exploits the pre-established conduit, collecting angular fragments of mafic foam and mingling with the remains of liquid basanite on the way to the surface

In both scenarios, the phonolite must have followed the basanite through its conduit. A comparable mechanism has been found in the Katmai region, Alaska. There, the default type of eruption has been described as coming from small, andesite magma chambers that experience mafic recharge. At low recharge vigour, the basalt mixes with the andesite. However, when unmixed mafic scoria is erupted, this is interpreted as basalt magma passing through the andesite chamber with limited interaction only (Coombs et al. 2000; Eichelberger and Izbekov 2000). At Montaña Reventada, the phonolite was probably rather cool prior to interaction, indicating a high viscosity body into which the basanite intruded, a Katmai-type scenario is therefore highly conceivable. The basanite would initially quench at the interface with the phonolite (mafic foam, type I inclusions, Fig. 11.8a). Type II inclusions would form when the reheated and partly re-mobilised phonolite would have started to enter the established basanite conduit, collecting the type I fragments (the former quench zone) and commencing

interaction with the liquid basanite magma that is left within the conduit. Because of the ongoing thermal interaction between the phonolite and the basanite, the temperature contrast progressively lowered, allowing for converging viscosities that increasingly permitted mingling to form the type III inclusions (Fig. 11.8b).

Equally plausible, however, is the notion that the basanite was blocked by the phonolite chamber, thereby partly intruding it, but eventually continuing to ascend to the side of it. Again, type I inclusions would have formed at initial contact, while type II and type III would have been generated when the re-heated phonolite exploited the basanite conduit afterwards. Examples for a similar scenario have been found at Karymsky (Kamchatka), Katmai/Novarupta centre (Alaska) and also the 2010 Eyjafjallajökull/Fimmvörðuháls eruption in Iceland, where mafic dykes first opened a fissure at the flank of these volcanoes before triggering more silicic eruptions from central vents (Eichelberger and Izbekov 2000; Gertisser 2010; Gudmundsson et al. 2010).

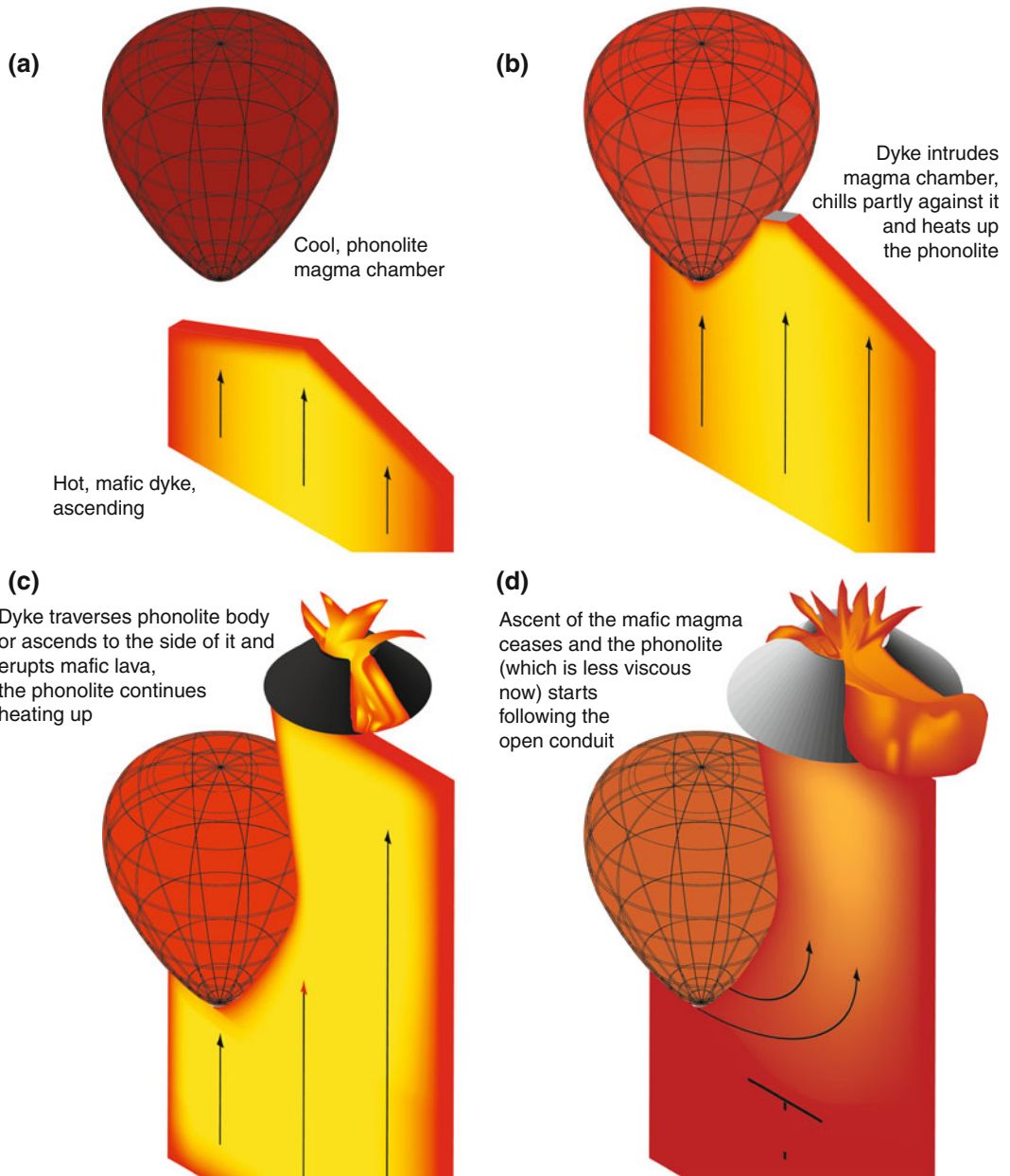


Fig. 11.9 3D Sketch of subsurface interaction between phonolite and basanite. Sketch of the envisaged subsurface dyke ascent and magma chamber dynamics. At Montaña Reventada, two possibilities of dyke ascent are conceivable; a basanite dyke taps a phonolite body peripherally, or a basanite dyke cuts through a cool phonolite magma chamber. **a** A mafic dyke encounters a

phonolite body in its ascent path. **b** The dyke taps the phonolite magma and initially quenches against it due to a large temperature contrast. **c** The dyke either intrudes the phonolite or cuts it peripherally and erupts before the phonolite. **d** The phonolite follows the basanite into its conduit after the basanite eruption wanes

For the reasons outlined, the interaction of a relatively small pocket of phonolite magma with a basanite dyke is envisaged at Montaña

Reventada (Fig. 11.9). The thermal contrast between cold phonolite and hot basanite inhibited hybridisation, and mixing only initiated

after some thermal equilibration had occurred. This interaction was limited to the remainders of the basanite dyke, which must have ceased erupting at that point.

11.6 Eruption Sequence

At Montaña Reventada, hybridisation remained incomplete as mixing was interrupted by eruption, and the inclusions reflect only short-term interaction between basanite and phonolite. However, prolonged interaction of basanite and phonolite would likely lead to homogenisation of the liquid magma portions and may be one of the processes responsible for producing intermediate magmas in the Canary archipelago and ocean islands elsewhere.

Most likely, a pre-existing phonolite magma pocket of the central Teide-Pico Viejo complex was cut by an ascending mafic dyke of the NW rift zone (Fig. 11.8a, b). From the isotopes it is evident that the phonolite had formed by processes that are unrelated to the basanite and the two magmas must have met just prior to eruption. The distinct Pb isotope signatures of basanite and phonolite magmas support the view that the two magmas were co-eruptive, but not co-genetic. When the basanite dyke intruded the phonolite magma chamber, it partly quenched against it, forming solidified, vesicular mafic inclusions within the phonolite. The subsequent entrainment of liquid basanite magma into the phonolite liquid gave rise to type II and III mafic inclusions that were locally hybridised by mingling and mineral exchange along with diffusion. Apart from the resulting hybrid inclusions, both end-members remained largely mechanically and chemically distinct.

The Montaña Reventada composite flow, therefore, is a direct manifestation of the petrogenetic bimodality in recent Tenerife activity. Reventada is located above the assumed boundary of the central Teide-Pico Viejo complex with the NW rift zone. In recent times, Teide and Pico Viejo have erupted phonolite from shallow magma chambers (below sea level, e.g., Ablay et al. 1998), whereas the rift zones

have continued to produce lavas of primitive composition that ascended in dykes from upper mantle or lower crustal levels (Carracedo et al. 2007). In the border zone between these two plumbing systems, not only Montaña Reventada shows a lower mafic and an upper felsic member, but so do the lavas of Cuevas Negras which also erupted successively during a single event (Carracedo et al. 2008). The Reventada eruption thus occurred in the transition zone between the central, phonolite-erupting Teide-Pico Viejo complex and the basanite-erupting NW rift zone, implying that two genetically distinct magmas have accidentally met to form this composite eruption.

References

- Ablay GJ, Carroll MR, Palmer MR, Martí J, Sparks RSJ (1998) Basanite-phonolite lineages of the teide-pico viejo volcanic complex, Tenerife, Canary Islands. *J Petrol* 39:905–936
- Abratis M, Schmincke H-U, Hansteen T (2002) Composition and evolution of submarine volcanic rocks from the central and western Canary Islands. *Int J Earth Sci* 91:562–582
- Araña V, Aparicio A, Garcia Cacho L, Garcia Garcia R (1989) Mezcla de magmas en la región central de Tenerife. In: Araña V, Coello J (eds) *Los Volcanes y La Caldera del Parque Nacional del Teide* (Tenerife, Islas Canarias). Serie Técnica, ICONA, pp 269–298
- Araña V, Martí J, Aparicio A, García-Cacho L, García-García R (1994) Magma mixing in alkaline magmas: an example from Tenerife, Canary Islands. *Lithos* 32:1–19
- Bacon CR (1986) Magmatic inclusions in silicic and intermediate volcanic rocks. *J Geophys Res* 91:6091–6112
- Bacon CR, Metz JM (1984) Magmatic inclusions in rhyolites, contaminated basalts, and compositional zonation beneath the Coso volcanic field, California. *Contrib Mineral Petrol* 85:346–365
- Bence AE, Albee AL (1968) Empirical correction factors for the electron microanalysis of silicates and oxides. *J Geol* 76:382–403
- Bindeman IN, Perchuk LL (1993) Experimental studies of magma mixing at high pressures. *Int Geol Rev* 35:721–733
- Bindeman IN, Davis AM (1999) Convection and redistribution of alkalis and trace elements during the mingling of basaltic and rhyolitic melts. *Petrol* 7:91–101

- Blake S (1981) Eruptions from zoned magma chambers. *J Geol Soc (London, UK)* 138:281–287
- Blake S, Ivey GN (1986) Magma-mixing and the dynamics of withdrawal from stratified reservoirs. *J Volcanol Geotherm Res* 27:153–178
- Calanchi N, Rosa R, Mazzuoli R, Rossi P, Santacroce R, Ventura G (1993) Silicic magma entering a basaltic magma chamber: eruptive dynamics and magma mixing—an example from Salina (Aeolian islands, Southern Tyrrhenian Sea). *Bull Volcanol* 55:504–522
- Campbell IH, Turner JS (1986) The influence of viscosity on fountains in magma chambers. *J Petrol* 27:1–30
- Carracedo JC, Rodríguez Badiola E, Guillou H, Paterne M, Scaillet S, Pérez Torrado FJ, Paris R, Fra-Paleo U, Hansen A (2007) Eruptive and structural history of Teide Volcano and Rift Zones of Tenerife, Canary Islands. *Geol Soc Am Bull* 119:1027–1051
- Carracedo JC, Rodríguez Badiola E, Guillou H, Paterne M, Scaillet S, Pérez Torrado FJ, Paris R, Rodríguez González A, Socorro S (2008) El Volcán Teide—Volcanología, Interpretación de Pasajes y Itinerarios Comentados. Caja General de Ahorros de Canarias
- Cas RAF, Wright JV (1987) Volcanic successions—modern and ancient. Allen & Unwin Ltd, London
- Coombs ML, Eichelberger JC, Rutherford MJ (2000) Magma storage and mixing conditions for the 1953–1974 eruptions of Southwest Trident volcano, Katmai National Park, Alaska. *Contrib Mineral Petrol* 140:99–118
- Coombs ML, Eichelberger JC, Rutherford MJ (2003) Experimental and textural constraints on mafic enclave formation in volcanic rocks. *J Volcanol Geotherm Res* 119:125–144
- De Campos CP, Dingwell DB, Perugini D, Civetta L, Fehr TK (2008) Heterogeneities in magma chambers: Insights from the behavior of major and minor elements during mixing experiments with natural alkaline melts. *Chem Geol* 256:131–145
- Eichelberger JC (1980) Vesiculation of mafic magma during replenishment of silicic magma reservoirs. *Nature* 288:446–450
- Eichelberger JC, Izbekov PE (2000) Eruption of andesite triggered by dyke injection: Contrasting cases at Karymsky Volcano, Kamchatka and Mt Katmai, Alaska. *Philos Trans R Soc London, Ser A* 358:1465–1485
- Eichelberger JC, Chertkoff DG, Dreher ST, Nye CJ (2000) Magmas in collision: rethinking chemical zonation in silicic magmas. *Geology* 28:603–606
- Freundt A, Schmincke H-U (1992) Mixing of rhyolite, trachyte and basalt magma erupted from a vertically and laterally zoned reservoir, composite flow P1, Gran Canaria. *Contrib Mineral Petrol* 112:1–19
- Geldmacher J, Haase KM, Devey CW, Garbe-Schönberg CD (1998) The petrogenesis of tertiary cone-sheets in Ardnamurchan, NW Scotland: petrological and geochemical constraints on crustal contamination and partial melting. *Contrib Mineral Petrol* 131:196–209
- Gertisser R (2010) Eyjafjallajökull volcano causes widespread disruption to European air traffic. *Geol Today* 26:94–95
- Gudmundsson MT, Pedersen R, Vogfjörd K, Thorbjarnardóttir B, Jakobsdóttir S, Roberts MJ (2010) Eruptions of Eyjafjallajökull Volcano, Iceland. *Eos Trans AGU* 91:190–191
- Gurenko AA, Hoernle KA, Hauff F, Schmincke H-U, Han D, Miura YN, Kaneoka I (2006) Major, trace element and Nd-Sr-Pb-O-He-Ar isotope signatures of shield stage lavas from the central and western Canary Islands: Insights into mantle and crustal processes. *Chem Geol* 233:75–112
- Hammer JE, Cashman KV, Voight B (2000) Magmatic processes revealed by textural and compositional trends in Merapi dome lavas. *J Volcanol Geotherm Res* 100:165–192
- Hawkesworth CJ, Blake S, Evans P, Hughes R, Macdonald R, Thomas LE, Turner SP, Zellmer G (2000) Time scales of crystal fractionation in magma chambers—integrating physical, isotopic and geochemical perspectives. *J Petrol* 41:991–1006
- Hibbard MJ (1995) Petrography to petrogenesis. Prentice Hall, Upper Saddle River
- Hildreth EW (1979) The bishop tuff: evidence for the origin of compositional zonation in silicic magma chambers. *Geol Soc Spec Publ* 180:43–75
- Huppert HE, Turner JS, Sparks RSJ (1982) Replenished magma chambers: effects of compositional zonation and input rates. *Earth Planet Sci Lett* 57:345–357
- Huppert HE, Sparks RSJ, Turner JS (1983) Laboratory investigations of viscous effects in replenished magma chambers. *Earth Planet Sci Lett* 65:377–381
- Huppert HE, Sparks RSJ, Turner JS (1984) Some effects of viscosity on the dynamics of replenished magma chambers. *J Geophys Res* 89:6857–6877
- Izbekov PE, Eichelberger JC, Ivanov BV (2004) The 1996 Eruption of Karymsky Volcano, Kamchatka: historical record of basaltic replenishment of an andesite reservoir. *J Petrol* 45:2325–2345
- Jellinek AM, Kerr RC, Griffiths RW (1999) Mixing and compositional stratification produced by natural convection 1. Experiments and their application to Earth's core and mantle. *J Geophys Res Solid Earth* 104:7183–7201
- Kouchi A, Sunagawa I (1985) A model for mixing basaltic and dacitic magmas as deduced from experimental data. *Contrib Mineral Petrol* 89:17–23
- Kuritani T (2001) Replenishment of a mafic magma in a zoned felsic magma chamber beneath Rishiri Volcano, Japan. *Bull Volcanol* 62:533–548
- Le Bas MJ, Maitre RWL, Streckeisen A, Zanettin B, ISotSol Rocks (1986) A chemical classification of volcanic rocks based on the total alkali-silica diagram. *J Petrol* 27:745–750
- Leshner CE (1986) Effects of silicate liquid composition in mineral-liquid element partitioning from soret diffusion studies. *J Geophys Res* 91:6123–6141
- Leshner CE, Walker D (1986) Solution properties of silicate liquids from thermal diffusion experiments. *Geochim Cosmochim Acta* 50:1397–1411
- Marshall LA, Sparks RSJ (1984) Origin of some mixed-magma and net-veined ring intrusions. *J Geol Soc (London, UK)* 141:171–182

- Merle O (1998) Internal strain within lava flows from analogue modelling. *J Volcanol Geotherm Res* 81:189–206
- Palacz ZA, Wolff JA (1989) Strontium, neodymium and lead isotope characteristics of the Granadilla Pumice, Tenerife: a study of the causes of strontium isotope disequilibrium in felsic pyroclastic deposits. *Geol Soc Spec Publ* 42:147–159
- Pallister JS, Hoblitt RP, Reyes AG (1992) A basalt trigger for the 1991 eruptions of Pinatubo volcano? *Nature* 356:426–428
- Perugini D, Poli G, Mazzuoli R (2003) Chaotic advection, fractals and diffusion during mixing of magmas: evidence from lava flows. *J Volcanol Geotherm Res* 124:255–279
- Simonsen SL, Neumann ER, Seim K (2000) Sr-Nd-Pb isotope and trace-element geochemistry evidence for a young HIMU source and assimilation at Tenerife (Canary Island). *J Volcanol Geotherm Res* 103:299–312
- Snyder D, Tait S (1996) Magma mixing by convective entrainment. *Nature* 379:529–531
- Sparks SRJ, Sigurdsson H, Wilson L (1977) Magma mixing: a mechanism for triggering acid explosive eruptions. *Nature* 267:315–318
- Stewart ML, Pearce TH (2004) Sieve-textured plagioclase in dacitic magma: Interference imaging results. *Am Mineral* 89:348–351
- Troll VR, Schmincke H-U (2002) Magma mixing and crustal recycling recorded in ternary feldspar from compositionally zoned peralkaline ignimbrite 'A', Gran Canaria, Canary Islands. *J Petrol* 43:243–270
- Troll VR, Donaldson CH, Emeleus CH (2004) Pre-eruptive magma mixing in ash-flow deposits of the Tertiary Rum Igneous Centre Scotland. *Contrib Mineral Petrol* 147(6):722–739
- Turner JS (1980) A fluid-dynamical model of differentiation and layering in magma chambers. *Nature* 285:213–215
- Turner JS, Campbell IH (1986) Convection and mixing in magma chambers. *Earth Sci Rev* 23:255–352
- Turner SP, Platt JP, George RMM, Kelley SP, Pearson DG, Nowell GM (1999) Magmatism associated with orogenic collapse of the betic-alboran domain, SE Spain. *J Petrol* 40:1011–1036
- Walker D, DeLong SE (1982) Soret separation of mid-ocean ridge basalt magma. *Contrib Mineral Petrol* 79:231–240
- Walker D, Leshner CE, Hays JF (1981) Soret separation of lunar liquids. Paper presented at the lunar and planetary science XII, 16–20 March
- Watson EB (1982) Basalt contamination by continental crust: Some experiments and models. *Contrib Mineral Petrol* 80:73–87
- Watson EB, Baker DR (1991) Chemical diffusion in Magmas: an overview of experimental results and geochemical applications. In: Perchuk LL, Kushiro I (eds) *Advances in physical geochemistry*, vol 6. Springer, New York, pp 120–151
- Wiesmaier S (2010) Magmatic differentiation and bimodality in oceanic island settings—implications for the petrogenesis of magma in Tenerife, Spain. PhD Thesis, Trinity College Dublin, Dublin
- Wiesmaier S, Deegan F, Troll V, Carracedo J, Chadwick J, Chew D (2011) Magma mixing in the 1100 AD Montaña Reventada composite lava flow, Tenerife, Canary Islands: interaction between rift zone and central volcano plumbing systems. *Contrib Mineral Petrol* 162:651–669
- Wolff JA, Storey M (1984) Zoning in highly alkaline magma bodies. *Geol Mag* 121:563–575
- Wolff JA, Grandy JS, Larson PB (2000) Interaction of mantle-derived magma with island crust? Trace element and oxygen isotope data from the Diego Hernandez Formation, Las Canadas, Tenerife. *J Volcanol Geotherm Res* 103:343–366
- Zimanowski B, Büttner R, Koopmann A (2004) Experiments on magma mixing. *Geophys Res Lett* 31:L09612